FIRST INVESTIGATION OF AN ALL-FIBER VERSATILE LASER FREQUENCY REFERENCE AT 2 μM FOR CO_2 LIDAR APPLICATIONS

S. Schilt[1,*], K. Hey Tow[2], R. Matthey[1], M. Petersen[1], L. Thévenaz[2], T. Südmeyer[1]
[1]*Laboratoire Temps-Fréquence, Université de Neuchâtel, Av. de Bellevaux 51, CH-2000 Neuchâtel, Switzerland*
[2]*EPFL Swiss Federal Institute of Technology, Institute of Electrical Engineering, SCI-STI-LT, Station 11, CH-1015 Lausanne, Switzerland*

**e-mail: stephane.schilt@unine.ch*

I. INTRODUCTION

Nowadays, space-borne differential absorption lidar (DIAL) instruments are under investigation by space agencies to monitor the integrated column density or the atmospheric density profile of gaseous species from space to ground. A species of particular interest in the context of greenhouse gases and global climate warming is CO_2. Two wavelength ranges at 1572 nm and 2051 nm are being considered for a future CO_2 space-borne integrated-path DIAL (IPDA) instrument [1]; the former range is technologically more mature while the latter is more favourable from a spectroscopic point-of-view [2]. The performance of such systems is notably determined by the spectral purity, accuracy and frequency stability of a low-power continuous-wave laser that seeds the pulsed laser transmitter.

An IPDA system operates at two different on-line and off-line wavelengths. The on-line wavelength is generally detuned from the center of the probed molecular absorption line with a frequency offset that favours the monitoring of CO_2 in the lower troposphere, where its mixing ratio variability is of high interest. A precise control of the frequency detuning of the seed laser is thus needed in a spectral range covering a few GHz around the center of the transition. Simultaneously, high stability and good accuracy of the laser frequency are required. At 1572 nm, the targeted frequency stability (in terms of Allan deviation) of 20 kHz above 700-s integration time was demonstrated [3], reaching values of 2 kHz at 1 s and < 800 Hz from 1 hour up to 3 days. This was achieved using a configuration with an electro-optic modulator (EOM) frequency comb bridging the spectral gap between a 1572-nm slave laser and a 1560-nm master laser, frequency-doubled and locked to a Rb transition [4]. The achieved frequency stability of the master and slave lasers coincided with the stability of similar Rb-stabilized lasers at 780 nm, so that the good frequency stability of Rb locking was efficiently transferred to the 1.56-μm spectral range. However, this approach cannot be immediately applied at 2051 nm. Therefore, a direct stabilization to a CO_2 transition is needed, which is weaker and spectrally-broader than the atomic Rb transition used in the aforementioned 1572-nm laser stabilization scheme.

Stabilizing a laser with a frequency detuning from the center of a molecular transition can be achieved using a side-of-fringe locking scheme, however the method suffers from its sensitivity to amplitude variations that are transposed to frequency fluctuations, and from the impossibility to precisely control the absolute offset frequency. Another common approach for a detuned locking is a master-slave configuration, in which a master laser is stabilized to the center of the considered transition, and a slave laser is offset-locked with respect to the master laser, achieved by a phase-lock loop or by a frequency offset-lock [5]. These methods have proven their efficiency to transfer the frequency stability of the master laser to the slave laser, but they need two distinct laser sources, each with its own driving electronics, which can be a drawback in some conditions, e.g., for space applications.

We present, here, a different approach to frequency-stabilize a laser with an offset frequency from the center of a CO_2 transition at 2051 nm based on a versatile modulation sideband locking scheme enabling the laser to be directly locked at an adjustable frequency detuning, without using a master-slave configuration. Since parameters like weight and size are of prime importance for space applications, a hollow-core photonic crystal fiber (HC-PCF) filled with a low pressure (~20 mbar) of pure CO_2 and sealed at both ends by splices to silica fibers is used as a compact gas reference cell. This enables an all-fiber set-up to be implemented, which is robust and mechanically-stable. First, we will describe the general principle of our frequency locking scheme (Section II), then we report in Section III some experimental results related to various aspects of the developed laser frequency reference and locking system (FRLS).

II. EXPERIMENTAL SET-UP

A. Modulation Sideband Locking Scheme

In order to stabilize a laser in the vicinity of the R(30) transition in the $(4\nu_2 + \nu_3)$ vibrational band of CO_2 at 2051 nm with a precisely controlled frequency detuning, we have developed a modulation sideband locking scheme based on the principle displayed in Fig. 1. It consists in modulating a singlemode distributed feedback (DFB) fiber-coupled laser (Nanoplus) using a broadband intensity EOM (Photline) to generate a pair of sidebands, one of which being stabilized to the center of the CO_2 transition using a feedback loop. The frequency of the laser carrier can, therefore, be precisely set by changing the frequency used to generate the sidebands, thereby locking it at the target frequency detuning. The stabilization of the sideband is performed by wavelength modulation spectroscopy (WMS) [6], implemented by applying a sinusoidal frequency modulation to the EOM driving signal, supplied by a voltage-controlled oscillator (VCO). An error signal is obtained by demodulating the optical signal transmitted through a reference gas cell at the VCO modulation frequency. A feedback signal for laser stabilization is finally applied to the laser injection current.

This stabilization method is very generic and can be applied to other molecular species at different wavelengths in the near-infrared. One of its major benefits is a modulation-free laser carrier. A narrow-linewidth stable laser signal is thus available at the output of the system, e.g., for further injection locking of a DIAL pulsed transmitter. Another relevant aspect of this method is its capability to make a self-contained off-center line locking, i.e., without the use of an auxiliary laser locked at the line center.

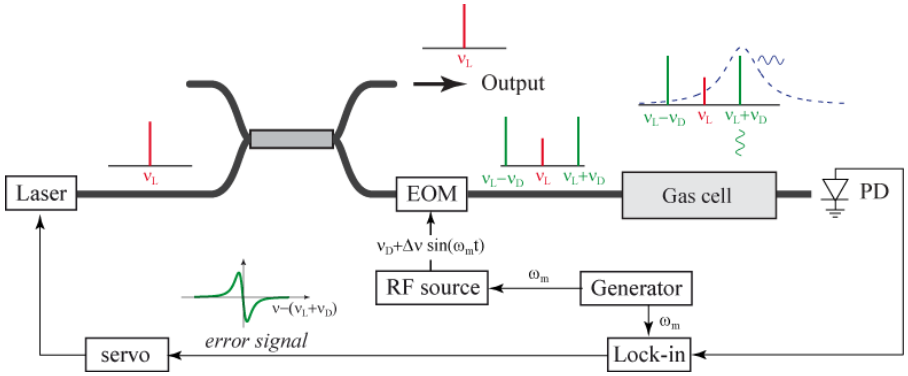

Fig. 1. Schematic representation of the modulation sideband locking for off-center stabilization of a laser emitting at frequency ν_L to a molecular transition. Modulation sidebands are created using an EOM, with a frequency separation corresponding to the targeted detuning ν_D from the absorption line center. PD: photo-detector; ω_m: modulation frequency; $\Delta\nu$: frequency modulation amplitude.

B. Fabrication of HC-PCF Reference Gas Cells

Regarding space applications, parameters such as the weight, size, ruggedness, or insensitivity to vibrations, are of prime importance. Holey fibers, more particularly hollow-core fibers, are excellent medium to create light-gas interactions in a very confined medium. In these micro-structured fibers, light is not guided by total internal reflection as in standard optical fibers, but by a photonic bandgap in the cladding that acts like a barrier for light [7]. As the guiding mechanism is no longer dependent on the core refractive index, it is possible to design fibers that guide light in a hollow core, so that most of the optical power (generally > 95%) does not propagate in the silica matrix, but in the core medium (generally air). Filling the hollow core with a specific gas enables the realization of very compact reference cells with long optical pathlengths in a small form factor. However, HC-PCFs also present some drawbacks such as (i) intermodal interference noise resulting from the simultaneous propagation of several optical modes for HC-PCFs with a core diameter compatible with standard singlemode (SM) fibers, (ii) the difficulty to be fusion-spliced to standard silica fibers owing to the high sensitivity of the thin silica web to heating, or (iii) the presence of interferometric noise caused by back-reflections at both ends of the HC-PCF that result from the large refractive index contrast between silica and air when an HC-PCF is spliced to SM fibers to make a sealed gas cell.

The fabrication process of the all-fiber CO_2 cell is schematized in Fig. 2. It relies on the permeation of gaseous helium through the walls of the silica fiber [8] to fabricate low-pressure gas cells that can be sealed by a fusion splice realized at ambient pressure conditions without contamination of the cell by the surrounding air. One end of the HC-PCF is first connectorized by a fusion splice to a SM fiber pigtail. The "pigtailed" HC-PCF is then placed in a hermetic vacuum chamber equipped with optical fiber and electrical feedthroughs enabling the HC-PCF filling process to be monitored on-line by a spectroscopic measurement with a laser source tuned to an absorption line of the gas species. Light is injected into the HC-PCF through the connectorized end and the transmitted light is monitored at the HC-PCF output with a free-space photodetector. Air in the chamber is then evacuated with a vacuum pump to purge the fiber. After the purging process, the vacuum chamber is loaded with CO_2 at the desired filling pressure (20-30 mbar in our case). The CO_2 molecules slowly diffuse into the HC-PCF core through its open end. Once the HC-PCF is filled with CO_2 at the targeted low pressure (which takes a few hours depending on the HC-PCF length and core diameter), the chamber is filled with a high pressure of pure helium (over atmospheric pressure), which rapidly diffuses into the HC-PCF core. The fiber thus contains a mixture of CO_2 diluted in a high helium pressure. At this stage, the gas chamber can be opened since air contamination into the HC-PCF core is prevented by the helium overpressure, which will take several minutes to diffuse out of the fiber when exposed to atmospheric conditions. This gives sufficient time to seal the bare end of the HC-PCF by splicing it to a SM fiber. Once the CO_2-filled gas cell is hermetically sealed on both ends, the helium gradually permeates out through the thin silica fiber within a couple of hours, leaving behind only the low pressure of pure CO_2 in the HC-PCF core.

Based on previous works on wavelength modulation spectroscopy [9], enhanced modelling and simulations were performed to quantify the important aspects of the modulation sideband locking technique. They showed that the targeted frequency stability of <100 kHz at an integration time of 10 s appears achievable using a fiber cell of a few meters length (typically 3 m) filled with a low pressure of CO_2 (typically 20 mbar), yielding an optical transmission at linecenter of ~19% and an absorption profile linewidth (FWHM) of ~450 MHz. Therefore, several 3-m long gas cells with 20-mbar targeted CO_2 pressure were fabricated using a commercially-available HC-PCF with a core diameter of 14.5 µm (HC-2000-01, NKT Photonics). During the filling process the value of the peak transmission was observed to saturate after about 80 minutes, indicating that the HC-PCF core was completely filled with CO_2. This duration is in good agreement with the filling time of 78 minutes that was estimated using an analytical diffusion model developed at EPFL [10] and the parameters of the HC-PCF.

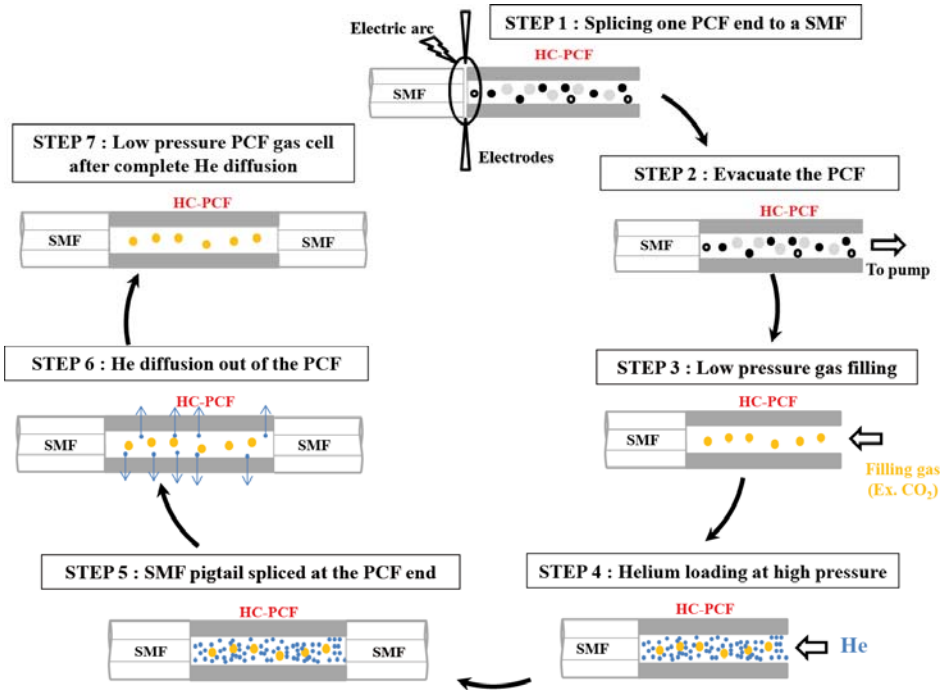

Fig. 2. Applied procedure for the fabrication of a fibered low-pressure gas cell based on an HC-PCF. Polarization maintaining or multimode fibers can also be used instead of SM fibers (SMF) for sealing the cell and coupling light into and out of the HC-PCF.

III. EXPERIMENTAL RESULTS

A. HC-PCF CO_2 Cell Characterization

The first fabricated fiber gas cells made use of standard SM fibers to seal the cell input and output ports (SM-SM configuration). Spectroscopic measurements showed an absorption profile of the CO_2 R(30) transition with a linewidth (FWHM) in the range of 420 to 750 MHz and a relative absorption at linecenter between 63% and 86%. The variability of these values likely resulted from an imprecise control of the CO_2 pressure in the vacuum chamber. The overall optical transmission of these cells (out of any CO_2 absorption line) reached less than 40%, limited by the splicing losses at the cell input and output. As illustrated in Fig. 3, an important interferometric noise pattern was present in the transmission spectra of these SM-SM cells, which was highly sensitive to temperature changes. In addition, this pattern turned out to depend on the polarization of the light coupled into the HC-PCF. Another contribution to the wavelength-dependent background of the HC-PCF cell resulted from a spatial filtering effect at the interface between the multimode HC-PCF and the SM output fiber.

To mitigate the impact of the interferometric noise in the cell transmission spectrum, HC-PCF gas cells were manufactured using two different sealing fibers: a polarization-maintaining (PM) fiber at the cell input and a multimode (MM) fiber at the cell output (PM-MM configuration). This geometry reduces the two aforementioned contributions to the cell transmission background. This led to a reduction of its peak-to-peak amplitude by a factor higher than 2 (see Fig. 3). In addition, the use of the MM fiber at the output port significantly improved the overall transmission of the gas cell up to 70%. Finally, it is worth noticing that for each gas cell, comparison of the transmission spectra recorded at an interval of more than one year did not reveal observable changes in the cell parameters, indicating that the tightness of the fiber cells is not compromised.

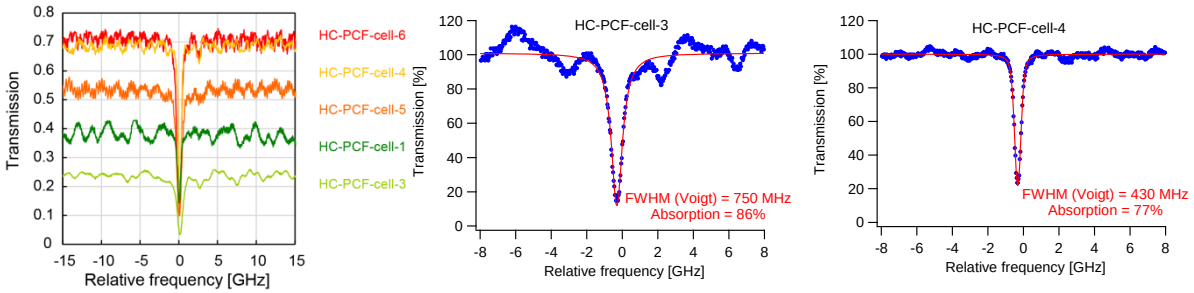

Fig. 3. Transmission spectrum of various realizations of HC-PCF cells in the vicinity of the CO_2 R(30) transition at 2.051 μm. Cells 1 and 3 are sealed with SM fibers at both input and output ports, while cells 4, 5 and 6 are sealed with a PM input fiber and a MM output fiber. (left) Overall cell transmission, including splicing losses and fiber attenuation. (center and right) Measured relative transmission (blue points) and Voigt fit (red line) of two HC-PCF gas cells of different geometries: SM-SM (center) and PM-MM (right) configurations.

B. Error Signal Generation

The parameters of the intensity EOM (carrier frequency, RF input power and DC bias voltage) are adjusted in order to suppress the optical carrier and to produce a pair of sidebands of maximum amplitude with a frequency separation corresponding to twice the targeted frequency detuning of the laser from the center of the CO_2 transition. Fig. 4(a) illustrates the transmission spectrum of the CO_2 R(30) transition obtained when the EOM output spectrum was tuned through the absorption line, obtained by scanning the laser injection current, for different frequency spacing between the sidebands. In this case, the optical carrier was not completely suppressed as a result of the non-optimized DC bias voltage applied to the EOM. The error signal to stabilize one of the sidebands to the center of the CO_2 transition was obtained by frequency-modulating the sidebands (by modulating the input voltage of the VCO at a frequency of ~20 kHz in the present case), and by subsequently demodulating the photodiode signal at the output of the reference gas cell at the same frequency (1f demodulation). A derivative-like signal of the CO_2 absorption line was thus obtained for each sideband (see Fig. 4(b)); no spectral feature occurs at the optical carrier (even if it is incompletely suppressed), as it is not affected by the modulation.

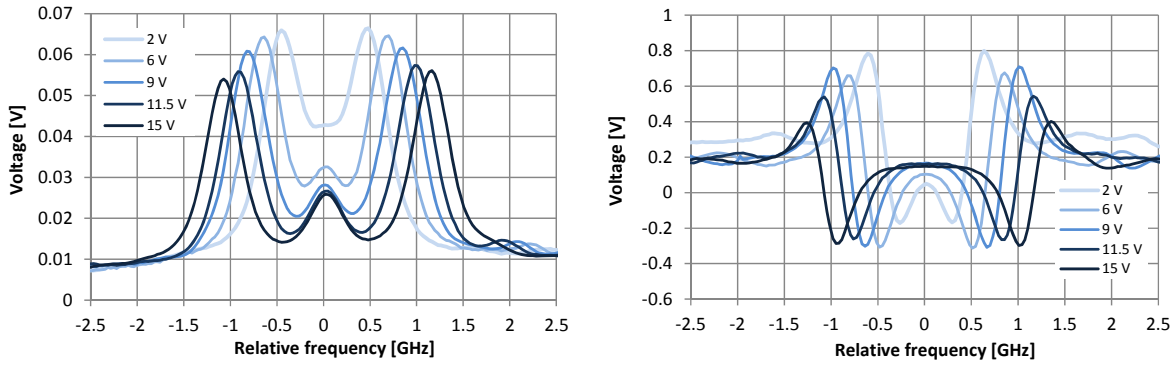

Fig. 4. Transmission spectrum (left) and error signal (right) of the modulation sideband method obtained for different sideband spacings (~460, 660, 820, 940 and 1100 MHz) achieved by changing the VCO control voltage and scanning the modulated laser through the CO_2 R(30) line. The DC bias voltage of the EOM was not optimized here, which explains the residual laser carrier observed in the center of the transmission spectra. However, the carrier has no contribution in the demodulated error signal (b) as it is not modulated.

C. Residual Amplitude Modulation Mitigation

An issue encountered with the implemented modulation sideband locking method is the offset present in the error signal (see Fig. 4(b)), which results from the residual amplitude modulation (RAM) of the EOM sidebands. The reason is the variation of the amplitude of the VCO that drives the EOM when its frequency is modulated via its control voltage. In order to reduce the impact of this RAM, we implemented a combination of a balanced optical detection with an active stabilization of the VCO output power.

For the balanced detection, a small fraction of the optical power was extracted before the HC-PCF gas cell using a fiber combiner and was detected by a reference photodiode. This reference signal was subtracted from the signal detected at the output of the HC-PCF. The common noise (power fluctuations resulting from the VCO modulation) between the two channels was strongly reduced in this way as illustrated in Fig. 5(a). However, the mitigation of the RAM effect with this balanced detection was incomplete, so that a complementary active control of the RF power driving the EOM was implemented to further reduce this effect.

In a first implementation, the VCO output power was controlled through its supply voltage and stabilized to an external reference voltage. The variations of the VCO output power were indirectly assessed from the optical power detected by the reference photodiode of the balanced detection to generate an error signal. This signal was amplified by a proportional-integral (PI) servo-controller and the resulting correction signal was applied to the supply voltage of the VCO. Fig. 5 (b) shows the RAM reduction achieved using this active stabilization, which is further increased when combined with the balanced detection (red trace in Fig. 5(b)).

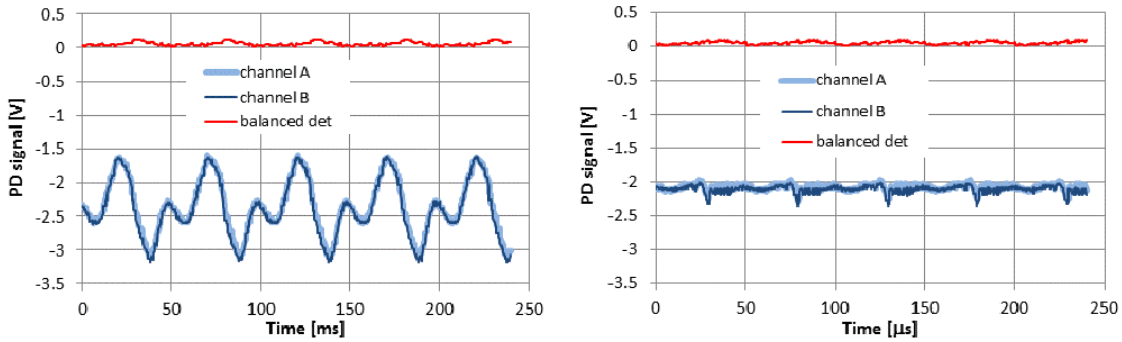

Fig. 5. Reduction of the RAM signal induced by the frequency modulation of the VCO using a balanced detection (left) and the combination of an active control of the VCO output power and a balanced detection (right). Channels A and B represent the signals at the output of the HC-PCF gas cell and in the reference channel, respectively.

The impact of the balanced detection and of the VCO stabilization on the error signal for laser sideband locking is displayed in Fig. 6. With the VCO stabilization, the offset in the 1*f* signal is strongly reduced, which is important to get a stable and accurate locking point of the laser. In addition, the error signal becomes more symmetric, which is also beneficial for the laser stabilization. In a next stage, we plan to implement this active stabilization using a high-bandwidth voltage-controlled attenuator to further improve the cancellation of the RAM effect.

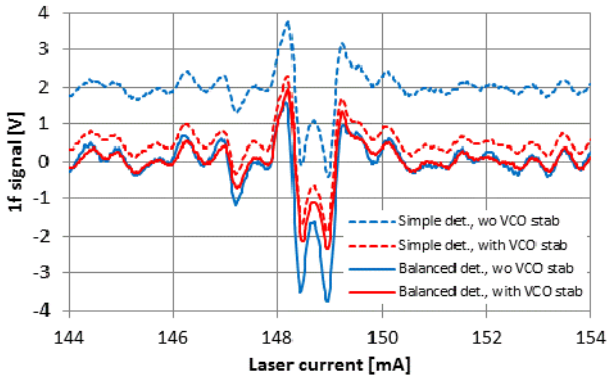

Fig. 6. Impact of the active control of the VCO output power on the error signal of an HC-PCF cell. Additional reduction of the RAM contribution is obtained using a balanced detection scheme. The horizontal axis represents the injection current of the laser used to scan the EOM spectrum through the CO_2 transition, with a tuning coefficient of ~2 GHz/mA.

D. Preliminary Evaluation of the Laser Frequency Stabilization

A preliminary evaluation of the modulation sideband locking has been performed. The upper EOM sideband was locked to the center of the CO_2 R(30) transition and the optical carrier was detuned by around 950 MHz (corresponding to the EOM drive frequency). The frequency stability of the locked laser was assessed from the heterodyne beat signal with a fully-stabilized Er:fiber optical frequency comb (Menlo Systems) referenced to an H-maser. The beat frequency, as well as the repetition rate and carrier-envelop offset frequency of the comb, were measured using a Π-type frequency counter without dead-time. The short-term frequency fluctuations of the laser are shown in Fig. 7, measured in free-running and locked conditions, with the corresponding Allan deviation. A frequency stability better than 100 kHz for averaging times 1 s < τ < 10 s, and slightly lower at longer averaging times, is obtained. This preliminary stability measurement was carried out using the first realized fiber gas cell (HC-PCF-cell-1, SM-SM configuration), which was affected by relatively large background fluctuations. Improvement of the frequency stability is expected in the future with the use of improved cells of the PM-MM configuration.

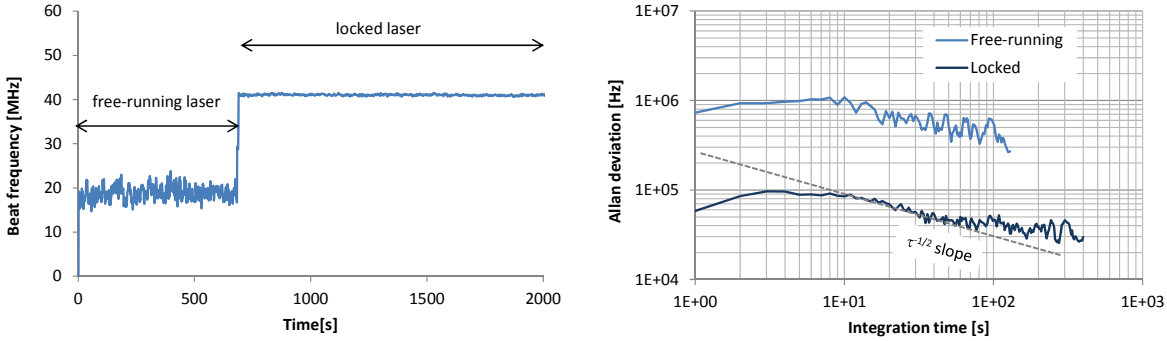

Fig. 7. (left) Frequency stability of the laser in free-running mode and locked to the side of the CO_2 R(30) transition using the cell HC-PCF-cell-1, which transmission spectrum is reproduced in Fig. 3. (right) Corresponding Allan deviation.

IV. CONCLUSION AND OUTLOOK

We have reported on our on-going work to develop a frequency-stable seed laser at 2051 nm for a CO_2 IPDA instrument. To enable the laser to be stabilized at an arbitrary detuning frequency from the center of the selected CO_2 R(30) transition, a modulation sideband locking scheme has been implemented with the use of an intensity EOM to create a pair of optical sidebands. By applying a frequency modulation to the sidebands, an error signal is generated for the stabilization of one of the sidebands to the center of the CO_2 transition. A stable frequency of the laser carrier is thus achieved, with a frequency detuning from the transition center frequency that is directly controlled by the EOM driving signal. The unmodulated stable optical carrier constitutes the output of the system to be used for further injection locking of a DIAL pulsed transmitter laser.

In order to realize an all-fiber set-up that is compact, robust and mechanically-stable, an HC-PCF filled at low CO_2 pressure was used as a reference gas cell. Different sealing fibres were tested to ensure the best performance of our HC-PCF cells. A configuration made of a PM fiber at the input port and a MM fiber at the output showed improved performance in terms of a smaller variations in the cell background transmission spectrum and a higher overall transmission resulting from smaller splicing losses.

A preliminary evaluation of the stabilized laser detuned by around 950 MHz from the center of the CO_2 R(30) transition showed that the targeted frequency stability of <100 kHz at an integration time of 10 s appears achievable using a fiber cell of 3-m length filled with 20 mbar of pure CO_2. Our next steps will be to improve the sideband stabilization and to perform a more detailed characterization of the laser performance, in terms of short- and mid-term stability, frequency accuracy and reproducibility.

ACKNOWLEGEMENTS

This work is funded by the European Space Agency (ESTEC contract No 4000108041/13/NL/PA).

REFERENCES

[1] S.R. Kawa, J. Mao, J.B. Abshire, G.J. Collatz, X. Sun, C.J. Weaver, “Simulation studies for a space-based CO_2 lidar mission,” *Tellus*, vol. 62B, pp. 759-769, 2010.

[2] G. Ehret, C. Kiemle, M. Wirth, A. Amediek, A. Fix, S. Houweling, “Space-borne remote sensing of CO_2, CH_4, and N_2O by integrated path differential absorption lidar: a sensitivity analysis,” *Appl. Phys. B*, vol. 90, pp. 593-608, 2008.

[3] R. Matthey, W. Moreno, F. Gruet, P. Brochard, S. Schilt, and G. Mileti, “Rb-stabilized laser at 1572 nm for CO_2 monitoring,” *Journal of Phys.: Conference Series*, vol. 723, 012034, 2016.

[4] R. Matthey, F. Gruet, S. Schilt, G. Mileti, “Compact rubidium-stabilized multi-frequency reference source in the 1.55-µm region,” *Opt. Letters*, vol. 40, pp. 2576-2579, 2015.

[5] S. Schilt, R. Matthey, D. Kauffmann-Werner, C. Affolderbach, G. Mileti, L. Thévenaz, “Laser offset-frequency locking up to 20 GHz using a low-frequency electrical filter technique,” *Appl. Optics*, vol. 47, pp. 4336-4344, 2008.

[6] J. M. Supplee, E. A. Whittaker, W. Lenth, “Theoretical description of frequency modulation and wavelength modulation spectroscopy,” *Appl. Optics*, vol. 33, pp. 6294–6302, 1994.

[7] R. F. Cregan, B. J. Mangan, J. C. Knight, T. A. Birks, P. St. J. Russell, P. J. Roberts, D. C. Allan, “Single-mode photonic band gap guidance of light in air”, *Science*, vol. 285, 1537, 1999.

[8] P. S. Light, F. Couny, and F. Benabid, “Low optical insertion-loss and vacuum-pressure all-fiber acetylene cell based on hollow-core photonic crystal fiber,” *Opt. Lett.*, vol. 31, pp. 2538-2540, 2006.

[9] S. Schilt, L. Thévenaz, P. Robert, “Wavelength modulation spectroscopy: combined frequency and intensity laser modulation,” *Appl. Opt.*, vol. 42, pp. 6728-6738, 2003.

[10] I. Dicaire, J.-C. Beugnot, L. Thévenaz, “Analytical modeling of the gas-filling dynamics in photonic crystal fibers,” *Appl. Opt.*, vol. 49, pp. 4604‑4609, 2010.